

A Combined Effect of Molecular Electrostatic Potential and N7 Accessibility Explains Sequence-Dependent Binding of *cis*-[Pt(NH₃)₂(H₂O)₂]²⁺ to DNA Duplexes**

Véronique Monjardet-Bas, Miguel-Angel Elizondo-Riojas,* Jean-Claude Chottard, and Jiří Kozelka*

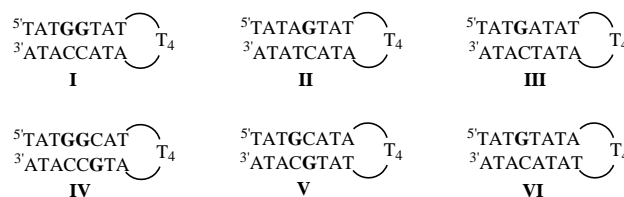
The sequence selectivity that characterizes the DNA binding of the antitumor drug cisplatin (*cis*-[PtCl₂(NH₃)₂]) has been subject to a number of investigations.^[1–8] The drug binds preferentially to guanine residues involved in G_n runs (*n* ≥ 2), where it forms N7–N7 intrastrand GG–Pt chelates as the major adducts. The species actually reacting with DNA are the hydrolyzed forms of cisplatin, namely, *cis*-[PtCl(NH₃)₂(H₂O)]⁺ (**1**) and/or *cis*-[Pt(NH₃)₂(H₂O)₂]²⁺ (**2**).



As the overall selectivity observed for the cisplatin–DNA interaction may arise from a combination of individual binding preferences of the two hydrolyzed species, our goal is to investigate the factors determining the kinetics of DNA binding of each complex. Understanding these factors should, on one hand, give us a clue to the overall sequence selectivity of cisplatin and, on the other hand, reveal the impact of exchanging a single ligand on the kinetics of platination. This latter point is interesting in the more general context of sequence-dependent binding of electrophiles to DNA.

Our strategy has been to examine the reactions of **1** and **2** with hairpin-stabilized duplex oligonucleotides in which one to three guanine residues are placed in different local sequences, while the overall environment is retained. Measuring the rate constants for platination of the individual

guanine residues of these duplexes enabled us to study the influence of the adjacent bases on the platination of a guanine within duplex DNA. For the diaqua species **2**, we have now measured the platination rate constants of all the guanines involved in the duplexes shown in Scheme 1. We demonstrate here that the rate constants determined for the individual



Scheme 1. Schematic representation of the hairpin-stabilized duplex oligonucleotides used in the reactions with **1** and **2**.

guanine residues can be accounted for by a kinetic model consisting of an initial, rapid, and reversible association of **2** on the surface of DNA and a subsequent irreversible ligand substitution step. Our model considers the molecular electrostatic potentials (MEP) and accessible areas (aa) of the van der Waals spheres of the N7 atoms as the principal variables determining the sequence-dependent reaction kinetics. It differs from the accessible surface integrated field (ASIF) model introduced earlier by Lavery and Pullman to interpret sequence-dependent N7-alkylation,^[9,10] which combined the influences of accessibility and electrostatics by calculating the flux of the electrostatic field through the accessible surface. In our model, electrostatics is considered mainly to affect the local concentration of the electrophile on the N7 van der Waals surface, whereas accessibility determines the kinetics of the proper ligand substitution step.

From the rate constants shown in Table 1, we infer that within duplex DNA, the reactivity of a guanine residue G towards **2** decreases in the series TGG > GGT > TGA ≈ AGT > GGC ≈ TGT > TGC. This order is similar to but not identical with the order of the MEP in the vicinity of the N7 atoms of G, as calculated for double-stranded B-DNA triplets:^[11] GGT > TGG > GGC > AGT > TGA ≈ TGT > TGC. This suggests that one component of the observed sequence selectivity of **2** may arise from different local concentrations of **2** on the DNA surface. A reversible association between the cationic complex **2** and the anionic DNA has been shown to precede ligand substitution.^[12] The substitution step is expected to proceed with its own sequence

Table 1. Apparent rate constants measured for the reaction of **2** with the individual guanine residues of the DNA duplexes shown in Scheme 1. The rate constants correspond to the underscored guanine.^[a]

Sequence	Duplex	<i>k</i> _{app} [M ^{−1} s ^{−1}]	Ref.
T <u>G</u> GT	I	18(1)	[7]
T <u>G</u> GT	I	15(1)	[7]
A <u>G</u> T	II	9(1)	[7]
T <u>G</u> A	III	9.6(5)	[19]
T <u>G</u> GC	IV	32(5)	[32]
T <u>G</u> GC	IV	2.0(5)	[32]
T <u>G</u> C	V	0.5(1) ^[b]	[32]
T <u>G</u> T	VI	1.9(5)	[19]

[a] Reaction conditions: 20 °C, 0.1 M NaClO₄, pH 4.5 ± 0.1. [b] Rate constant for each individual guanine residue.

[*] M.-A. Elizondo-Riojas⁺, Dr. J. Kozelka, V. Monjardet-Bas, Prof. J.-C. Chottard
Laboratoire de Chimie et Biochimie Pharmacologiques et Toxicologiques
UMR 8601 CNRS, Université René Descartes
45, rue des Saints-Pères, 75270 Paris (France)
Fax: (+33)1-4286-8387
E-mail: melizond@ccr.dsi.uanl.mx,
kozelka@biomedicale.univ-paris5.fr

[+] On leave from the Centro Universitario Contra el Cancer (CUCC)
Hospital Universitario “Dr. José Eleuterio González”
Universidad Autónoma de Nuevo León
Monterrey, N.L. (México)

[**] We are indebted to Johnson-Matthey, Inc. for a generous loan of cisplatin. Computer time from the IDRIS computer center of the CNRS and financial support from COST (project D8/0004/97), enabling scientific exchange with other research groups, are gratefully acknowledged. M.A.E.R. was the 1997 recipient of the Gemini Award from the International Precious Metals Institute (IPMI).



Supporting information for this article is available on the WWW under <http://www.angewandte.org> or from the author.

selectivity, and the ordering of the apparent rate constants is thus likely to correspond to a combination of the selectivities of both steps. The kinetics of the second step will depend on 1) the accessibility of the N7 atom and 2) its intrinsic reactivity, which is related to the stability of the transition state. The energy of the transition state is expected to be a function of the interactions between the platinum ligands and the neighboring DNA residues, and also of the MEP, which will influence the electrostatic component of the Pt–N7 bond being formed. In our work we have tested a hypothesis according to which the major factor determining the sequence dependence of the substitution step is the accessibility of the N7 center. We show in the following that a simple mathematical model combining the electrostatic effect in the association step with the accessibility effect in the substitution step indeed allows one to account for the observed rate constants.

The two-step mechanism that we considered is shown in Scheme 2. Since the reversible association step, driven by diffusion and electrostatic forces, is expected to be very fast,^[13] the apparent rate constant will be equal to the product of the equilibrium constant K and the rate constant k for the ligand substitution step. The local concentration of the cationic platinum complex in the vicinity of a given N7 atom is proportional to K , which is dependent on the local MEP. This dependence is accounted for by an exponential term derived from Boltzmann statistics, that is, $K \propto \exp(-q \text{MEP}(\epsilon_L RT)^{-1})$, where ϵ_L is the local dielectric coefficient, q is the unitless formal charge of the species reacting with DNA, and the MEP

as well as RT are expressed in kcal mol^{-1} . The rate constant k is considered to be proportional to the accessible area aa on the N7 van der Waals surface. Thus, the apparent rate constant is given by Equation (1), where c_1 is a proportionality factor

$$k_{\text{app}} = Kk = c_1 aa \exp(-q \text{MEP}(\epsilon_L RT)^{-1}) \quad (1)$$

with the dimensions of $\text{M}^{-1} \text{s}^{-1} \text{\AA}^{-2}$ which includes the rate constant for the proper chemical step (ligand substitution).

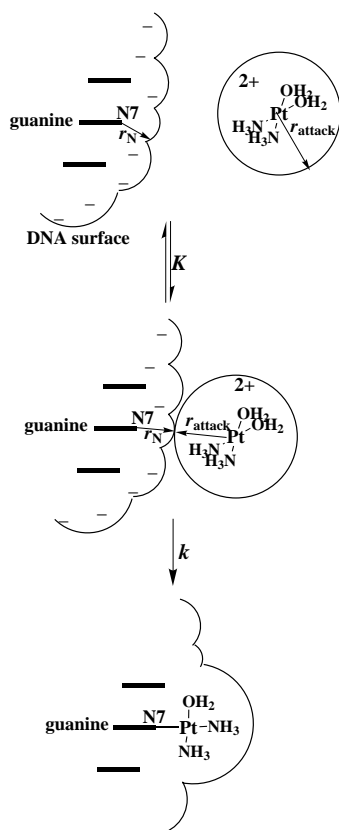
In this model, sequence-dependent effects on c_1 —resulting, for example, from nonbonding interactions in the transition state or from structural variations of the double helix—are not taken into account. Equation (1) can be transformed into Equation (2).

$$\ln(k_{\text{app}} aa^{-1}) = \ln(c_1) - q \text{MEP}(\epsilon_L RT)^{-1} = c'_1 + c'_2 \text{MEP} \quad (2)$$

The constants c'_1 and c'_2 can be obtained by plotting $\ln(k_{\text{app}} aa^{-1})$ against MEP (by using the observed rate constants listed in Table 1 for k_{app} and the calculated values for aa and MEP) and determining the regression line. The aa and MEP values were calculated for each guanine environment by using B-DNA model structures, as outlined in the Experimental Section. In these calculations, the reacting platinum complex was approximated as a sphere of radius r_{attack} (Scheme 2) that is considered to roll over the DNA van der Waals surface.^[9,14] The MEP values associated with each aa were determined for the point on the bisector of the C5–N7–C8 angle having a distance of $(r_{\text{attack}} + r_N)$ from N7 (r_N is the van der Waals radius of the N atom).

Both aa and MEP were calculated for the interval $3.8 \text{\AA} \leq r_{\text{attack}} \leq 5 \text{\AA}$. The lower limit corresponds to the radius of a spherical van der Waals envelope of complex **2** and the upper limit to that of an envelope of complex **2** associated axially with two molecules of water.^[15] Within the interval considered for r_{attack} , the MEP values undergo approximately linear parallel shifts; thus, only those calculated for one selected value of r_{attack} (4.9\AA) are shown in Figure 1 a. In contrast, the variations of the accessible areas upon increasing r_{attack} are clearly nonlinear (Figure 1 b) and the relative order changes. In order to find out for which r_{attack} Equations (1) and (2) work the best, we have plotted $\ln(k_{\text{app}} aa^{-1})$ against MEP and carried out a linear regression corresponding to Equation (2) for each considered value of r_{attack} . The root-mean-square (rms) deviation between the left- and right-hand sides of Equation (2), determined with the optimized values for c'_1 and c'_2 over the eight rate constants listed in Table 1, was plotted against r_{attack} (see the Supporting Information). The best fit is obtained for $r_{\text{attack}} = 4.88 \text{\AA}$. Deconvolution of the optimized value of $-0.14 \text{ mol kcal}^{-1} \text{K}^{-1}$ for c'_2 into $-q(\epsilon_L RT)^{-1}$ ($q = 2$, $R = 0.002 \text{ kcal mol}^{-1} \text{K}^{-1}$, $T = 293 \text{ K}$) yields an ϵ_L value of about 24, which seems reasonable for a short-distance interaction at the DNA surface. The observed k_{app} values are plotted against the calculated values (right-hand side of Equation (1) with $c_1 = 9.57 \text{ M}^{-1} \text{s}^{-1} \text{\AA}^{-2}$ and $\epsilon_L = 24.4$, as optimized for $r_{\text{attack}} = 4.88 \text{\AA}$) in Figure 2. It can be seen that the fit is fairly satisfactory.

Sequence-selective electrophilic attack on guanine N7 centers of DNA has been observed for N7-methylation with



Scheme 2. The two-step mechanism considered in the mathematical model.

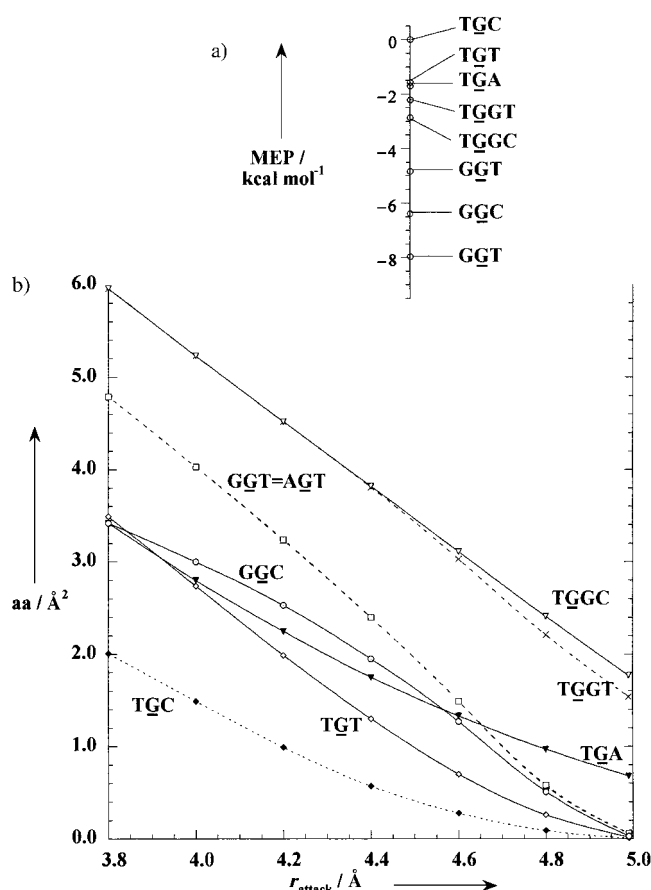


Figure 1. a) The molecular electrostatic potentials calculated for guanine residues in the sequences of the duplexes shown in Scheme 1 at $r_{\text{attack}} = 4.9 \text{ \AA}$ (see the Experimental Section and Scheme 2). The MEP value for TGC was set arbitrarily to zero. b) Accessible areas aa around N7 atoms calculated as a function of r_{attack} for the same sequences.

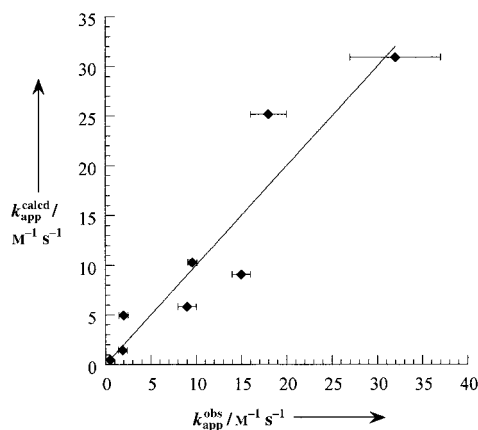


Figure 2. Observed apparent rate constants k_{app} (from Table 1) for the reactions between the individual guanine residues of the DNA duplexes shown in Scheme 1 and complex **2**, plotted against values calculated by using Equation (1), with the optimized constants $c_1 = 9.57 \text{ M}^{-1} \text{ s}^{-1} \text{ \AA}^{-2}$ and $\epsilon_L = 24.4$. The aa and MEP values were calculated with $r_{\text{attack}} = 4.88 \text{ \AA}$.

nitrogen mustards.^[16] For the least bulky nitrogen mustard, mechlorethamine, the relative rates of methylation roughly correlate with the MEP calculated at the N7 lone pair. For methylation of tRNA^{Phe} with dimethylsulfate, Lavery and Pullman found that a reactivity index combining steric and electrostatic factors, called accessible surface integrated field

(ASIF), yields a qualitative correlation with relative methylation rates of individual guanines of tRNA^{Phe}.^[9]

For DNA platination, we^[7,17] and others^[18] have previously suggested that hydrogen bonds between platinum ligands and DNA residues in the transition state could be responsible for the observed sequence selectivity. However, our later attempts to correlate the rate constants listed in Table 1 with the energies calculated for the corresponding pentacoordinate transition states were unsuccessful.^[19] The results presented here suggest that the main factors determining the sequence dependence of DNA platination with **2** are electrostatic potential and accessibility, while effects of noncovalent interactions in the transition state are probably of secondary importance. Hydrogen bonds from platinum ligands certainly do influence the reaction kinetics, as the reactivity of complexes $\text{cis-}[\text{PtL}(\text{NH}_3)_2(\text{H}_2\text{O})]^{n+}$ ($n = 1, 2$) towards a given DNA guanine residue increases with increasing hydrogen bonding capacity of the ligand L.^[7] However, as our present results suggest, and also in agreement with recent model calculations by Hambley,^[20] these interactions may be rather sequence-unspecific. For example, sequence-neutral hydrogen bonds from the platinum ligands to the 5'-phosphodiester group probably favor the approach of the platinum complex to any guanine N7 site, as indicated by the fact that a 5'-phosphate accelerates the platination of guanine nucleotides^[21,22] and dinucleotides.^[23]

The way our kinetic model accounts for electrostatic effects is principally different from Lavery's ASIF approach used to quantify the rate of guanine methylation by CH_3^+ cations generated from dimethylsulfate.^[9] The ASIF model considers the rate constant to be proportional to the flux of the electrostatic field through the accessible surface fragment of the van der Waals sphere around the N7 atom. In this model, the crucial variable is the radial component of the electric field at the center of the attacking sphere rolling over the van der Waals surface. We have calculated the sequence-dependent variations of this component within the interval $3.8 \text{ \AA} \leq r_{\text{attack}} \leq 5 \text{ \AA}$ and found them to be rather small ($\leq 13\%$) and almost independent of r_{attack} (not shown). Thus, multiplication of each accessible surface element with the radial field component modifies the sequence dependence of the accessible area around N7 only slightly. As a result, we found that the correlation of the experimental rate constants (Table 1) with the ASIF values is not better than that with the accessible areas only. At variance with ASIF, our present model considers that the electrostatic forces mainly determine the local concentration of the cationic species at the DNA surface, which depends on the MEP, a scalar entity. The corresponding function, $\exp(-q \text{MEP}(\epsilon_L RT)^{-1})$, undergoes sequence-dependent variations up to a factor of 6. Thus, the influence of electrostatics on the rate constant is significantly more important in our model than in the ASIF model.

As already mentioned, the MEP is expected to affect not only the preassociation equilibrium constant K but also the rate constant k for the substitution step, since a large electron density at the N7 lone pair will strengthen the Pt–N7 bond being formed. Thus, the exponential term in Equation (1) may contain some influence of the MEP on k , even though the refined ϵ_L value of 24 agrees reasonably well

with what would be expected for an outer-sphere preassociation.

Some striking features of the sequence-selective binding of **2** to DNA (Table 1) can now be interpreted on the basis of our kinetic model. First, the very low reactivity of the TGC sequence seems to be a combined effect of the steric bulk exerted by the flanking pyrimidines and of the low negative MEP. Second, the high reactivities of TGG and GGT are apparently also a combined effect of that of high aa and highly negative MEP. Finally, the similar reactivities of TGA and AGT towards **2** appear to originate from a compensation between the higher negative MEP of AGT and a higher accessibility of TGA. Interestingly, this compensation occurs only at $r_{\text{attack}} > 4.65 \text{ \AA}$, since below this value both aa and MEP favor AGT (Figure 1). Size and charge of the attacking species are therefore expected to affect selectivity.

In conclusion, the sequence dependence of guanine N7 platination with complex **2** can be accounted for by a combined effect of the molecular electrostatic potential, considered in our kinetic model to determine the local concentration of **2** at the DNA surface, and the steric bulk of the neighboring bases, quantified as the accessible area of the van der Waals sphere around the N7 atom. The good fit that we obtain between calculated and experimental rate constants suggests that other effects, such as nonbonding interactions in the transition state, are less important. This result is interesting for two reasons. First, it indicates that accessibility is a main factor determining the sequence-dependent binding of platinum complexes to DNA. This is further supported by our preliminary results showing that the same kinetic model holds also for the N7 platination by the monocationic complex **1**. Second, our model delineates a concept of treating the influence of electrostatics and accessibility in a simple mathematical formula which is formally in accord with the two-step mechanism (Scheme 2) generally accepted for ligand exchange reactions on metal complexes.^[24] This concept may be applicable—with eventual extensions, for example, to include the effects of solvation on the MEP^[25,26] or the influence of sequence-dependent variations of DNA structure on both the MEP and aa^[10]—to other metal complex–DNA systems, and possibly to DNA alkylation by organic electrophiles as well.

Experimental Section

The accessible areas (aa) around guanine N7 atoms and the associated molecular electrostatic potential (MEP) were calculated for the duplex parts of the hairpins shown in Scheme 1; canonical Arnott B-DNA structures were constructed by using the NUCGEN module of AMBER,^[27] and the helices were truncated on both sides after the third base pair from the central G–C base pair. (Thus, the calculations were carried out on double-stranded DNA heptamers.) The principle of the determination of aa has been outlined by Lavery and Pullman.^[9,28] Briefly, the reacting complex is approximated by a sphere of a radius r_{attack} which is considered to roll over the van der Waals surface of the molecule. The accessible area is defined as the surface that the center of the sphere describes while the sphere is in contact with the van der Waals sphere of the N7 atom; aa was calculated by using the Korobov method^[29] to generate a regular distribution of points on a sphere of the radius $(r_{\text{N7}} + r_{\text{attack}})$ around the selected N7 atom. (We used a Korobov index of 26, generating 196418 points.) Subsequently, we employed the algorithm by Lavery and Pullman^[9] to check for each point whether it lay within the van der Waals distance

$(r_{\text{X}} + r_{\text{attack}})$ of any atom X. The fraction of points outside all van der Waals contacts multiplied with $4\pi(r_{\text{N}} + r_{\text{attack}})^2$ finally yielded aa. The MEP was calculated for the space point at the C5–N7–C8 bisector at the distance $r_{\text{N}} + r_{\text{attack}}$ from the N7 atom (r_{N} is the van der Waals radius of N), as the sum $332\sum q_i/r_i$ [kcal mol^{−1}] calculated over all atoms, q_i [e] being the charge of atom i and r_i its distance from the space point in Å. For convenience, all MEP values were shifted so as to set the MEP for TGC to zero. (This offset modifies c_1 and c_1' but not c_2' or ϵ_L .)

The MEP and aa values plotted in Figure 1 were determined using the van der Waals radii and ESP atomic charges of Lavery and Pullman.^[28] Alternative use of van der Waals radii and/or atomic charges from the AMBER force field^[30] or of van der Waals radii by Bondi^[31] modified the numerical aa and MEP values but did not appreciably affect their sequence dependence.

Received: February 1, 2002

Revised: May 13, 2002 [Z18628]

- [1] F. Reeder, J. Kozelka, J.-C. Chottard, *Inorg. Chem.* **1996**, *35*, 1413–1415.
- [2] F. Reeder, F. Gonnet, J. Kozelka, J. C. Chottard, *Chem. Eur. J.* **1996**, *2*, 1068–1076.
- [3] S. J. Berners-Price, K. J. Barnham, U. Frey, P. J. Sadler, *Chem. Eur. J.* **1996**, *2*, 1283–1291.
- [4] S. K. C. Elmroth, S. J. Lippard, *Inorg. Chem.* **1995**, *34*, 5234–5243.
- [5] F. Legendre, J. Kozelka, J.-C. Chottard, *Inorg. Chem.* **1998**, *37*, 3964–3967.
- [6] M. S. Davies, S. J. Berners-Price, T. W. Hambley, *J. Am. Chem. Soc.* **1998**, *120*, 11380–11390.
- [7] F. Legendre, V. Bas, J. Kozelka, J.-C. Chottard, *Chem. Eur. J.* **2000**, *6*, 2002–2010.
- [8] M. S. Davies, S. J. Berners-Price, T. W. Hambley, *Inorg. Chem.* **2000**, *39*, 5603–5613.
- [9] R. Lavery, A. Pullman, *Biophys. Chem.* **1984**, *19*, 171–181.
- [10] S. Furois-Corbin, B. Pullman, R. Lavery, *Int. J. Quantum Chem. Quant. Biol. Symp.* **1984**, *1984*, 273–286.
- [11] A. Pullman, B. Pullman, *Quart. Rev. Biophys.* **1981**, *14*, 289–380.
- [12] Y. Wang, N. Farrell, J. D. Burgess, *J. Am. Chem. Soc.* **2001**, *123*, 5576–5577.
- [13] H. Strehlow, *Rapid Reactions in Solution*, VCH, Weinheim, **1992**, p. 18.
- [14] B. Lee, F. M. Richards, *J. Mol. Biol.* **1971**, *55*, 379–400.
- [15] J. Kozelka, J. Bergès, R. Attias, J. Fraitaig, *Angew. Chem.* **2000**, *112*, 204–207; *Angew. Chem. Int. Ed.* **2000**, *39*, 198–201.
- [16] K. W. Kohn, J. A. Hartley, W. B. Mattes, *Nucl. Acids. Res.* **1987**, *15*, 10531–10549.
- [17] A. Laoui, J. Kozelka, J.-C. Chottard, *Inorg. Chem.* **1988**, *27*, 2751–2753.
- [18] T. W. Hambley, *Inorg. Chem.* **1991**, *30*, 937–942.
- [19] V. Monjardet-Bas, Ph.D. thesis, Université Paris VI, Paris, **2001**.
- [20] T. W. Hambley, *J. Chem. Soc. Dalton Trans.* **2001**, 2711–2718.
- [21] A. B. Robins, *Chem. Biol. Interactions* **1973**, *6*, 35–45.
- [22] A. T. M. Marcelis, C. Erkelens, J. Reedijk, *Inorg. Chim. Acta* **1984**, *91*, 129–135.
- [23] J.-P. Girault, J.-C. Chottard, G. Chottard, J.-Y. Lallemand, *Biochemistry* **1982**, *21*, 1352–1356.
- [24] H. Strehlow, *Rapid Reactions in Solution*, VCH, Weinheim, **1992**, p. 116.
- [25] B. Jayaram, K. A. Sharp, B. Honig, *Biopolymers* **1989**, *28*, 975–993.
- [26] B. Honig, A. Nicholls, *Science* **1995**, *268*, 1144–1149.
- [27] D. Pearlman, D. A. Case, J. W. Caldwell, W. S. Ross, T. E. Cheatham, D. M. Ferguson, G. L. Seibel, U. C. Singh, P. K. Weiner, P. A. Kollman, *Amber 4.1*, University of California, San Francisco, **1995**.
- [28] R. Lavery, A. Pullman, B. Pullman, *Int. J. Quantum Chem.* **1981**, *20*, 49–62.
- [29] A. H. Stroud in *Digital Computer User's Handbook* (Eds.: M. Kleen, G. A. Korn), McGraw-Hill, New York, **1967**.
- [30] T. E. Cheatham III, P. Cieplak, P. A. Kollman, *J. Biomol. Struct. Dyn.* **1999**, *16*, 845–862.
- [31] A. Bondi, *J. Chem. Phys.* **1964**, *68*, 441–451.
- [32] V. Monjardet-Bas, J.-C. Chottard, J. Kozelka, *Chem. Eur. J.* **2002**, *8*, 1144–1150.